Synthesis of hybrid nanowire arrays and their application as high power supercapacitor electrodes†

Manikoth M. Shaijumon,[ab] Fung Suong Ou,[ab] Lijie Ci[ab] and Pulickel M. Ajayan*[ab]

Received (in Cambridge, UK) 17th January 2008, Accepted 29th February 2008
First published as an Advance Article on the web 27th March 2008
DOI: 10.1039/b800866c

Arrays of multi-segmented hybrid nanostructures of carbon nanotube and gold nanowires have been synthesized using a combination of chemical vapour deposition and electrodeposition methods and we further demonstrate that ultra-high power electrochemical double layer capacitors can be engineered using these hybrid nanowires, resulting in very high power densities.

Electrochemical capacitors with their high power density and long cycle life will be important players in various energy storage devices.[1,2] The performance characteristics of electrochemical double layer capacitors (EDLCs) are fundamentally determined by the structural and electrochemical properties of electrodes.[2] They have been examined with great interest for their applications in hybrid vehicles and backup power supplies.[2–7] For such applications, it is extremely important to develop supercapacitors with higher power densities than are currently available.

Various materials including metal oxides,[8] doped conducting polymers,[9] and carbon[10] in different forms have been used as electrode materials. Metal oxide (*e.g.* RuO_2, MnO_2, IrO_2, Co_3O_4, MoO_3, WO_3 and TiO_2) based capacitors show very high specific capacitance and high specific power, but they are limited by their high cost. Electronically conducting polymers (ECPs) are less expensive, but they have poor reusability during cycling. Porous carbon materials have high surface area,[10] however, the low conductivity of porous carbon limits it from having high power densities. Excellent electrical properties and high surface areas of carbon nanotubes have attracted a great deal of attention and they have been used as electrodes for supercapacitors.[11–14] In spite of having ideal properties, CNT based supercapacitors do not meet the expected performance.[2] One of the major issues of CNT based supercapacitors is the high contact resistance between the electrode and the current collector which limits their performance.[3,5,13] Various methods have been employed to reduce the internal resistance of the CNT electrode for achieving high power capabilities.[3,5,6,13] A two-step process using a treated Al current collector has been shown to improve the Al/active material interface properties, thus decreasing the internal resistance.[6] Contact resistance could be lowered by growing CNTs directly on to a conductive substrate.[15,16] However, such bulk contacts still seem to be uneven and considerable contact resistance is observed between the substrate and the electrode. All these methods are multi-step and are shown to have only limited improvements in the supercapacitor performance. Hence, it is important to develop more versatile and modified electrodes that allow better contact between the metal and the nanotube structures. Recently we have developed a process for the synthesis of hybrid nanostructures of CNTs and metal nanowires.[17] Here, we report a technique to fabricate ultra-high power supercapacitors by using multi-segmented CNT/AuNW hybrid structures as electrodes. Both the electrode (CNTs) and current collector (AuNW) are integrated into a single nanostructured wire thus resulting in excellent performance for our supercapacitors, with a very high power density of 48 kW kg^{-1}, which is much higher than the reported values for CNT-based supercapacitors. The intimate contact between metal and CNTs reduces the contact resistance and enhances its power capabilities.

The experimental procedure for growing CNT/AuNW hybrid structures is shown in Fig. 1 (see ESI† for details). Au nanowires are first grown inside the channels of commercially available AAO templates (nanopore diameter of ~200 nm and length of ~50 μm) using electrodeposition. After the electrodeposition of the Au nanowires, CVD was carried out to grow multi-walled carbon nanotubes (MWNTs) inside the template, by the pyrolysis of acetylene at 650 °C for 1–2 h with a flow of gas mixture containing Ar (85%) and C_2H_2 (15%) at a rate of 35 ml min^{-1}. The presence of an evaporated metal film prevents the CNT/AuNW hybrid structures from collapsing after the removal of templates.

Fig. 2 shows the SEM and TEM images of CNT/AuNW hybrid structures after removal of the template. CNT/AuNW

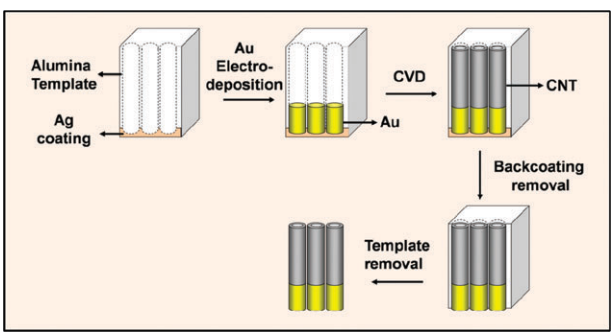

Fig. 1 Schematic showing the fabrication of CNT/AuNW hybrid structures inside the AAO template.

[a] *Department of Mechanical Engineering & Materials Science, Rice University, 6100, Main Street, Houston, Texas 77005, USA*
[b] *Department of Materials Science & Engineering, Rensselaer Polytechnic Institute, Troy, New York 12180, USA. E-mail: ajayan@rice.edu; Fax: +1 713-348-5423; Tel: +1 713-348-5904*
† Electronic supplementary information (ESI) available: Experimental details, characterization. See DOI: 10.1039/b800866c

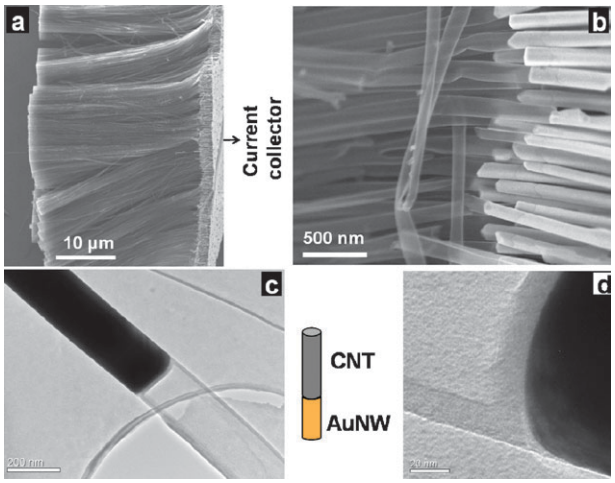

Fig. 2 (a) SEM image showing the CNT/AuNW segments and the Cu back layer. (b) High resolution SEM image showing the interface between the CNT and AuNW segments. (c) TEM image clearly showing the CNT/AuNW interface. The inner diameter of the CNT is approximately 170 nm. (d) HRTEM image showing the graphitic walls of CNT, approximately 15 nm thick. A schematic of a single hybrid nanowire is shown.

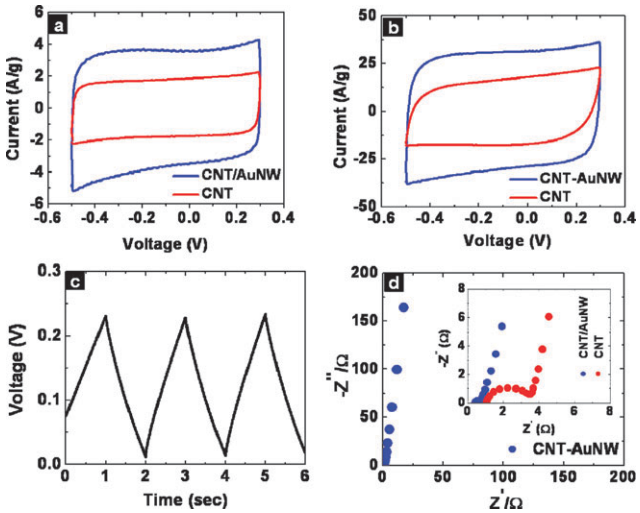

Fig. 4 Cyclic voltammograms measured at scan rates of (a) 100 mV s^{-1} and (b) 1000 mV s^{-1}, using 6 M KOH electrolyte. (c) Galvanostatic charge–discharge behavior measured at a constant current of 2 A g^{-1} for supercapacitor using CNT/AuNW electrodes. (d) Nyquist plots for the CNT/AuNW and CNT electrodes at an AC amplitude of 10 mV. Inset shows an enlarged scale.

hybrid nanowires are uniform and re-align even after removal of the AAO template. The two segments can be seen clearly in the image due to different contrast of gold and CNTs. The Au segment is typically grown about 3 μm in length, while the CNTs are about 40 μm, as shown in the SEM images (Fig. 2a and b). A spot profile EDX spectrum clearly shows a significant amount of gold from the brighter part (Fig. S1, ESI†). TEM image (Fig. 2 c) clearly indicates that the multi-walled carbon nanotube is nicely fused with the gold nanowire, forming a well adhered interface. The inner diameter of CNT was ~170 nm, with a wall thickness of ~15 nm (Fig. 2d).

These hybrid nanowires were dispersed in solvent by sonication for the TEM sample preparation and do not break, clearly indicating the robustness of these structures. Flexible films of CNT/AuNW hybrid structures obtained after the removal of templates in 3 M NaOH solution were directly used as electrodes in an electrochemical supercapacitor device. Two such films bonded back-to-back make a single supercapacitor device (Fig. 3). The Au segment of each electrode in contact with the Cu layer acts as the current collector.

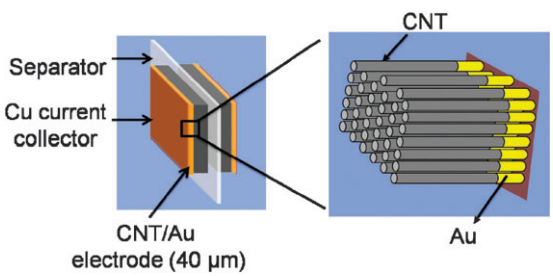

Fig. 3 Schematic diagram showing the supercapacitor device with CNT/AuNW electrodes. The Au segment of each electrode in contact with the Cu layer acts as the current collector.

The electrochemical properties and capacitive behavior of the supercapacitor electrodes (Fig. 4) were studied by cyclic voltammetry (CV), galvanostatic charge–discharge and impedance spectroscopy measurements. The specific capacitance was calculated from galvanostatic charge–discharge measurements. In order to compare the supercapacitor performance of our CNT/AuNW hybrid electrodes with CNTs, electrochemical measurements were also carried out for the supercapacitor devices with AAO template-grown CNT electrodes where a thermal evaporated metal layer acted as the current collector. Fig. 4a shows the CV behavior of the supercapacitor with CNT/AuNW and CNT electrodes using 6 M KOH electrolyte, with a sweep rate of 100 mV s^{-1} (see ESI† for details, Fig. S2). The CV curves for supercapacitor electrodes with CNT/AuNW hybrid structures present a rectangular shape, indicative of excellent capacitance properties. The pure CNT electrodes show lower performance. As evidenced by the slope of V/I at the rectangular sides in the CV curves, low equivalent series resistance (ESR) exists between the AuNW and the CNT in comparison to the pure CNT electrodes. Such low ESR is mainly due to the lower contact resistance between the current collector and the electrode, since ESR arises from the resistance of the electrode, electrolyte and the contact resistance between the electrodes and current collectors.[2] Large internal resistance generally results in distorted CV behavior, resulting in a narrower loop, at higher scan rates. However, supercapacitor electrodes using CNT/AuNW hybrid structures show rectangular CVs with close to ideal capacitive behavior, even at very high scan rates of 1000 mV s^{-1}, which again indicates a low ESR (Fig. 4b). Galvanostatic charge–discharge measurements were used to calculate the specific capacitance of the device. The constant current charge–discharge curves for CNT/AuNW electrodes (Fig. 4c) show typical ideal capacitive behaviour with very sharp responses, without any IR drop, this also suggests the low contact resistance in our

electrodes. The calculated specific capacitances were 72 and 38 F g^{-1}, respectively, for CNT/AuNW hybrid electrodes and CNT electrodes. Both CNT/AuNW and CNT electrodes were shown to possess good stability over 1000 charge–discharge tests. Fig. 4d presents the Nyquist plot of CNT/AuNW and CNT electrodes. CNT electrodes show a straight line in the low-frequency region and a semi-circle in the high frequency region (see inset of Fig. 4d), indicating that the supercapacitor is more resistive at high frequencies. The vertical shape at lower frequencies indicates pure capacitive behavior, representative of the ion diffusion in the porous structure of the electrode.[18] It is interesting to see that the semi-circle almost disappears in the Nyquist plot for the CNT/AuNW hybrid electrode due to extremely small contact resistance. The ESRs measured are 480 mΩ and 3.4 Ω for CNT/AuNW and CNT electrodes, respectively. Low ESR mainly results from the extremely small contact resistance, hence leading to efficient power density. This is obvious from the Nyquist plots (Fig. 4d), since both the electrodes show similar capacitive behavior, indicative of the ion mobility in the micropores.[18] However, the high frequency arc, which is attributed to the impedance resulting from the resistance between carbon particles and the backing current,[19] is almost negligible for CNT/AuNW hybrid electrodes. Excellent performance of a supercapacitor device with CNT/AuNW electrodes has been realized from its high power density. A maximum power density of 48 kW kg^{-1} is obtained at room temperature, for a supercapacitor device with CNT/AuNW electrodes, which is much higher than the reported values for carbon nanotube based supercapacitor devices.[4,5] For supercapacitors using CNT electrodes (with a thermal evaporated metal current collector), a maximum power density of 18 kW kg^{-1} has been reported. This highlights the influence of the interface resistance between current collector and active material on the performance of the supercapacitor. The large improvement in power density for CNT/AuNW electrodes, compared to CNT electrodes, could be attributed to low contact resistance arising from the well adhered interface between the CNT and AuNW junctions. Here, each carbon nanotube is electrically connected to the gold nanowire current collector, so that all the nanotubes contribute to the capacity there by improving the rate capabilities.

To conclude, we have synthesized arrays of CNT/AuNW multi-segmented hybrid structures *via* a template method. The CNT/AuNW hybrid electrodes showed excellent electrochemical performance with a maximum power density of $\sim$48 kW kg^{-1} which is attributed to the well adhered interface between CNT and AuNW segments. This results in nanoscale contact with each electrode and the current collector, leading to very low contact resistance. The 3-dimensional nanotubular electrode configuration results in improved electrolyte penetration. The new device configuration involves a simple electrode fabrication procedure and also helps in efficient packing.

The authors acknowledge support from the New York State Office of Science, Technology and Academic Research (NYSTAR). F.S.O. thanks Applied Materials Inc. for a graduate fellowship. M.M.S. is thankful to Dr A. Kumar for his valuable suggestions.

Notes and references

1 B. E. Conway, *Electrochemical Capacitors: Scientific Fundamentals and Technological Applications*, Kluwer, The Netherlands, 1999.
2 A. Burke, *J. Power Sources*, 2000, **91**, 37.
3 C. Portet, P. L. Taberna, P. Simon and E. Flahaut, *J. Electrochem. Soc.*, 2006, **153**, A649.
4 D. N. Futaba, K. Hata, T. Yamada, T. Hiraoka, Y. Hayamizu, Y. Kakudate, O. Tanaike, H. Hatori, M. Yumura and S. Iijima, *Nat. Mater.*, 2006, **5**, 987.
5 C. Du, J. Yeh and N. Pan, *Nanotechnology*, 2005, **16**, 350.
6 C. Portet, P. L. Taberna, P. Simon, E. Flahaut and C. Laberty-Robert, *Electrochim. Acta*, 2005, **50**, 4174.
7 A. S. Arico, P. Bruce, B. Scrosati, J. M. Tarascon and W. Van Schalkwijk, *Nat. Mater.*, 2005, **4**, 366.
8 (*a*) C. C. Hu, K. H. Chang, M. C. Lin and Y. T. Wu, *Nano Lett.*, 2006, **6**, 2690; (*b*) T. Cottineau, M. Toupin, T. Delahaye, T. Brousse and D. Belanger, *Appl. Phys. A: Mater. Sci. Process.*, 2006, **82**, 599; (*c*) J. P. Zheng and T. R. Jow, *J. Electrochem. Soc.*, 1995, **142**, L6.
9 M. Mastragostino, C. Arbizzani and F. Soavi, *Solid State Ionics*, 2002, **148**, 493.
10 (*a*) H. Shi, *Electrochim. Acta*, 1996, **41**, 1633; (*b*) J. Chmiola, G. Yushin, Y. Gogotsi, C. Portet, P. Simon and P. L. Taberna, *Science*, 2006, **313**, 1760; (*c*) E. Frackowiak and F. Beguin, *Carbon*, 2001, **39**, 937.
11 (*a*) C. M. Niu, E. K. Sichel, R. Hoch, D. Moy and H. Tennent, *Appl. Phys. Lett.*, 1997, **70**, 1480; (*b*) S. Sarangapani, B. V. Tilak and C.-P. Chen, *J. Electrochem. Soc.*, 1996, **143**, 3791; (*c*) R. J. Brodd, K. R. Bullock, R. A. Leising, R. L. Middaugh, J. R. Miller and E. Takeuchic, *J. Electrochem. Soc.*, 2004, **151**, K1; (*d*) E. Frackowiak and F. Beguin, *Carbon*, 2002, **40**, 1775; (*e*) V. Pushparaj, M. M. Shaijumon, A. Kumar, S. Murugesan, L. Ci, R. Vajtai, R. Linhardt, O. Nalamasu and P. M. Ajayan, *Proc. Natl. Acad. Sci. U. S. A.*, 2007, **104**, 13574.
12 G. L. Che, B. B. Lakshmi, E. R. Fisher and C. R. Martin, *Nature*, 1998, **393**, 346.
13 K. H. An, W. S. Kim, Y. S. Park, J.-M. Moon, D. J. Bae, S. C. Lim, Y. S. Lee and Y. H. Lee, *Adv. Funct. Mater.*, 2001, **11**, 387.
14 (*a*) K. H. An, K. K. Jeon, J. K. Heo, S. C. Lim, D. J. Bae and Y. H. Lee, *J. Electrochem. Soc.*, 2002, **149**, A1058; (*b*) E. Frackowiak, K. Metenier, V. Bertagna and F. Beguin, *Appl. Phys. Lett.*, 2000, **77**, 2421.
15 (*a*) J. H. Chen, W. Z. Li, D. Z. Wang, S. X. Yang, J. G. Wen and Z. F. Ren, *Carbon*, 2002, **40**, 1193; (*b*) S. Talapatra, S. Kar, S. K. Pal, R. Vajtai, L. Ci, P. Victor, M. M. Shaijumon, S. Kaur, O. Nalamasu and P. M. Ajayan, *Nat. Nanotechnol.*, 2006, **1**, 112.
16 B. J. Yoon, S. H. Jeong, K. H. Lee, H. S. Kim, C. G. Park and J. H. Han, *Chem. Phys. Lett.*, 2004, **388**, 170.
17 F. S. Ou, M. M. Shaijumon, L. Ci, D. Benicewicz, R. Vajtai and P. M. Ajayan, *Appl. Phys. Lett.*, 2006, **89**, 243122.
18 W. C. Chen, T. C. Wen and H. S. Teng, *Electrochim. Acta*, 2003, **48**, 641.
19 Y. R. Nian and H. S. Teng, *J. Electrochem. Soc.*, 2002, **149**, A1008.